

UC San Diego

UC San Diego Electronic Theses and Dissertations

Title

MicroRNA analysis of human embryonic stem cell derived cardiomyocytes and neonatal rat ventricular cardiomyocytes

Permalink

<https://escholarship.org/uc/item/1sz5z8c5>

Author

Nelson, Brandon John

Publication Date

2007

Peer reviewed|Thesis/dissertation

UNIVERSITY OF CALIFORNIA, SAN DIEGO

MICRORNA ANALYSIS OF HUMAN EMBRYONIC STEM CELL DERIVED
CARDIOMYOCYTES AND NEONATAL RAT VENTRICULAR
CARDIOMYOCYTES

A Thesis submitted in partial satisfaction of the requirements for the degree Master
of Science

in

Biology

by

Brandon John Nelson

Committee in charge:

Professor Mark Mercola, Chair
Professor Michael David
Professor Immo Scheffler

2007

The Thesis of Brandon John Nelson is approved:

Chair

University of California, San Diego

2007

TABLE OF CONTENTS

Signature Page..... iii

Table of Contents.....iv

List of Figures.....v

List of Tables.....vi

List of Graphs.....vii

Acknowledgements.....viii

Abstract.....ix

Introduction.....1

Chapter 1--MicroRNA Profiling of hESC Derived Cardiomyocytes

 Abstract.....8

 Introduction.....8

 Materials and Methods.....9

 Results.....14

 Discussion.....19

Chapter 2--MicroRNA Analysis of Notch Activated Neonatal Rat Ventricular Cardiomyocytes

 Abstract.....21

 Introduction.....21

 Materials and Methods.....23

 Results.....24

 Discussion.....32

Chapter 3--Optimization of an High-Throughput Method of Transfection to Introduce Synthetic MicroRNAs into Neonatal Rat Ventricular Cardiomyocytes

 Abstract.....36

 Introduction.....36

 Materials and Methods.....37

 Results.....38

 Discussion.....42

Chapter 4--Final Discussion.....43

References.....45

List of Figures

Figure 1: Representation showing puromycin resistance being driven by the cardiomyocyte specific α -MHC promoter and Neomycin resistance being driven by the undifferentiated marker Rex (A). Time-course depiction for the differentiation of the hESC H9 line to the cardiomyocyte lineage (B). Day 55 puromycin selected cardiosphere, brightfield image (C).....	11
Figure 2: Invitrogen representation of the microarray used for the microRNA expression studies.....	12
Figure 3: Representative heat-map showing global changes across various time-points of cardiomyocyte differentiation. Cardiomyocytes were isolated at day 19, 29 and 40. Embryoid bodies were harvested at day 2, 8, 10 and 14 of differentiation. Embryoid bodies contain multiple lineages in addition to cardiomyocytes.....	13
Figure 4: Activity of recombinant hJagged1 on surface of Ad-hJagged1 infected NRCFs. Infected NRCFs were co-cultured with Hes-1 luciferase or mutant Hes-1 luciferase in transfected HeLa cells and luciferase activity was plotted relative to Ad-N ₂ ICD-infected HeLa cells as a positive control...	25
Figure 5: Neonatal Rat Cardiac Fibroblasts infected with Ad-GFP-hJagged1. Stained 48 hours after infection. (i) DAPI; (ii) eGFP; (iii) anti-hJagged1; (iv) Merge.....	28
Figure 6: HeLa cells stained for Notch 2 (i) DAPI; (II) anti-Notch2; (iii) Merge.....	28
Figure 7: Validation of DharmaFect3 as a transfection reagent for NRVCs (A); Histogram depicting the transfection efficiency of DharmaFect3 based upon the observed GAPDH knock-down in NRVCs by means of a siRNA to GAPDH (B); Representative staining of NRVCs for GAPDH and DAPI (C).....	40
Figure 8: Validation of Lipofectamine 2000 as transfection reagent for NRVCs and NRCFs (A); Bar-graph depicting the transfection efficiency of Lipofectamine 2000 based upon the observed GAPDH knock-down in NRVCs and NRCFs in response to transfection with a siRNA to GAPDH (B). Representative staining of NRVCs and NRCFs for GAPDH expression and DAPI (C).....	41
Figure 9: Summary of various transfection reagents compared by their transfection efficiency and toxicity.....	41

List of Tables

Table 1: Upregulated miRs relative to undifferentiated hESC H9. miRs in red have been shown to be expressed in adult mouse heart. Where the fold change is in red, this denotes that the miR has changed significantly in mouse models of cardiac hypertrophy in response to trans-aortic constriction.....	16
Table 2: Downregulated miRs relative to undifferentiated hESC H9. miRs in red have been shown to be expressed in adult mouse heart. Where the fold change is in red, this denotes that the miR has changed significantly in mouse models of cardiac hypertrophy in response to trans-aortic constriction.....	17
Table 3: Fold change in miR expression relative to undifferentiated hESCs. Significance was determined by Students T-test ($p < 0.05$). miRs in red have been shown to be expressed in adult mouse heart. Where the fold change is in red, this denotes that the miR has changed significantly in mouse models of cardiac hypertrophy in response to trans-aortic constriction	31

List of Graphs

- Graph 1: Histogram comparing expression of common miRs between day 19, 29 and 40 in selected and isolated cardiomyocyte populations relative to undifferentiated hESCs. All fold change values were statistically significant ($p < 0.05$).....18
- Graph 2: Significant change in miRNRVCs were compared to data from Ad- β -gal infected NRVCs for significant change in expression. Data were background corrected normalized across entire experiment (Latin squares normalization). Fold change in miR expression was measured for each feature, statistical significance determined by students T-test and p-values assigned.....30

ACKNOWLEDGEMENTS

I would like to thank my advisor Dr. Mark Mercola for his advice and support over the past several years. His constantly positive and energetic attitude made the lab environment not only conducive to a high level of learning but also made it relaxed and very enjoyable.

I would also like to thank all of the members of the Mercola Lab for their advice and support on various parts of my project. Without their constantly positive advice and guidance, my career as a graduate student would have been much less fulfilling.

Lastly, I would like to thank the members of my thesis committee, Drs. Michael David and Immo Scheffler for taking the time to read my thesis and participate in its defense.

ABSTRACT OF THE THESIS

MICRORNA ANALYSIS OF HUMAN EMBRYONIC STEM CELL DERIVED
CARDIOMYOCYTES AND NEONATAL RAT VENTRICULAR
CARDIOMYOCYTES

by

Brandon John Nelson

Master of Science in Biology

University of California, San Diego, 2007

Professor Mark Mercola, Chair

Cardiovascular disease is the primary cause of morbidity and mortality in the United States. The majority of patients who survive an initial myocardial infarction (M.I.) do not have a positive prognosis due to the increased work load that is placed upon the heart and this is compounded by the inability to regenerate the lost myocardium. Heart failure therefore is at its essence a loss of cardiomyocytes. This

problem has stimulated an intense research effort to develop the means to replace the damaged or dead cardiomyocytes with transplanted cells, such as human Embryonic Stem Cell Derived Cardiomyocytes (hESCDCs) or through expansion of putative adult cardiomyocytes, progenitors or stem cells.

In the current study we utilized Invitrogen's microRNA (miR) microarrays to examine the miR profile of hESCDCs in order to identify novel miRs that regulate the process of differentiation to the cardiomyocyte lineage in addition to miRs that are involved in maintaining the proliferative capacity of immature hESCDCs. With the same tools we are also analyzing Neonatal Rat Ventricular Cardiomyocytes (NRVCs) that have been induced to re-enter the cell cycle through over-expression of components of the Notch pathway. Here, we are looking also for novel miRs that are involved in Notch replication of NRVC cell cycle, either as agonists or antagonists. Identification of such miRs could increase our understanding of cardiomyocytes cell cycle and might lead to strategies to increase the pool of cardiomyogenic cells for therapeutic purposes. From these microarrays, we have identified several miRs that are involved in the processes before mentioned and are therefore being characterized functionally by means of high throughput screens and other studies to determine relevant targets.

Introduction

In developed countries, coronary heart disease (CHD) related mortality and morbidity places an enormous burden on society not only because of the personal it inflicts but because of enormous financial costs. For example, an individual dies every minute, or over 450,000 deaths occur in a year due to the effects of CHD, and these deaths almost exclusively result from a myocardial infarction (M.I.), or heart attack. What is most striking about these statistics is that 90% of the risk associated with CHD is due to 9 modifiable risk factors, and 90% of cardiac events occur in individuals with at least one elevated risk factor. These include: smoking, high level of blood lipids, hypertension, diabetes, excessive obesity, having a sedentary lifestyle, excess alcohol consumption, low fiber intake and a high psychosocial index. Knowledge of these factors and the burden of CHD for society should motivate us to improve our daily habits[1].

Strikingly, of the 565,000 M.I.s that occur annually, 300,000 are recurrent[1]. Recurrent attacks are, in a large part, the result of the strain that the first M.I. has placed on the heart. Weakening of the heart is compounded by the limited ability of the heart to regenerate. Also, adult cardiomyocytes cannot replicate and the endogenous progenitor or stem cell population is insufficient to overcome the damage resulting from a M.I.[2-4]. Thus, the damaged heart is susceptible to cardiomyopathy and progression to heart failure.

Current clinical strategies can relieve vascular damage (e.g. angioplasty) but there is no therapy to replace cardiomyocytes short of heart transplantation. This lack

of myocardial therapy underlies progression of 68 % of MI patients 6 years after having their first MI, will become disabled due to heart failure[1]. The demand for donor hearts for transplantation far outweighs their availability. Taken together, these concerns have led to an intense search for a transplantable source of cardiomyocytes.

One such area of increasing importance is the potential use of hESC derived cardiomyocytes (hESCDCs) as a cell-based therapy to help replace and regenerate infarcted tissue that has formed as a result of a heart attack. This is due to that shortly after birth, human cardiomyocytes terminally differentiate and lose their proliferative capability and therefore are unable to regenerate the infarcted tissue[5]. There are new studies showing that there might be a cardiac stem-cell niche, however the stem cell proliferative capacity in such extreme cell death cases such as in a heart attack remain unanswered. There are still many hurdles that must be overcome before hESCDCs can be utilized to this end. For one, the process of differentiating hESCs to the cardiomyocyte lineage is still a spontaneous event, and the numbers of cells needed for transplantation far outweigh the production capabilities at this time. Another hurdle is the fact that the cardiomyocytes that are produced through the differentiation process is actually a heterogeneous population of different types of cardiomyocytes which include ventricular, atrial and nodal cells, in addition to all of the other cell types that arise from the spontaneous differentiation process[6]. Therefore, it is necessary to obtain a method where the individual populations of cardiomyocytes can be purified before these cells can be utilized as a therapy. Currently there are two methods that can be utilized to achieve

this goal: either separate the fractions of cell types through a percoll gradient or to genetically modify a hESC line to contain a selectable drug marker under the control of a cell lineage specific promoter[7]. Lastly, the cardiomyocytes that are obtained from this process are very immature in contrast to their adult ventricular cardiomyocyte counterparts. For example, the hESCDCs have no functional t-tubule system; their sarcoplasmic reticulum is highly underdeveloped; their sarcomeres are highly disorganized, and they have numerous varying morphologies, all in contrast to adult ventricular cardiomyocytes[5].

One potential source of cells is cardiomyocytes derived from human embryonic stem cells (hESCs). hESCs form all 3 germ layers and can form all cells of the body and therefore are a potential source of cells for therapies , models of genetic disorders, studies of functional genomics and for drug toxicity screens[5]. First produced in 1998, hESCs are derived from pre-implantation embryos that otherwise would be discarded from in-vitro fertilization clinics after the reproduction needs of patients have been met. Currently, there are more than 200 independently established hESC lines, but only a handful is available for research in the U.S. using federal funds and this plus the ethical issues surrounding the use of discarded human embryos continue to be a matter of debate.

hESC lines are able to be grown in an undifferentiated state for an indefinite period of time. Cultured appropriately, they maintain their normal karyotype and grow in tightly packed colonies with a high nucleus to cytoplasm ratio and form teratomas when injected into immunocompromised SCID mice. Also, they are positive for several cell-surface antigens which include SSEA-4 and 3, in addition to

expressing pluripotency related genes such as Oct-4 and Nanog[5]. hESCs are ideal as a model system since they can potentially yield all cell types in the body. Also the cell types that differentiate hold promise for transplantation, pending consideration of allergenic immune response issues.

Nuclear transfer or the recently described methods for creating hESC-like cells from patients' own dermal fibroblasts, could potentially circumvent the need for immunosuppressive therapy. Cell-based transplantation therapy would be particularly valuable for degenerative disorders involving tissues with a limited capacity to regenerate, such as cardiac tissue or nervous tissue that was damaged due to neurodegenerative diseases or injury. Other types of ailments that hESCs holds promise for include: Alzheimer's disease, Parkinson's disease, stroke, diabetes, arthritis and burn trauma. Several challenges remain, however, before the promise of hESC based therapies can be realized. Perhaps most important is that directed differentiation of the pluripotent hESC to a clinically useful cell remains inefficient. Spontaneous differentiation to cardiomyocytes, for example, results in only a few percent of cardiomyocytes in the heterogeneous hESC culture. Therefore, the process of directed differentiation to a specific cell type must be fully understood to be able to produce a large, homogenous population of cells that can be subsequently used for these cell-based therapies.

Currently, there are several methods available to spontaneously induce hESCs to differentiate towards the cardiac lineage. One such method is to differentiate the cells in suspension as three-dimensional structures termed embryoid-bodies (EBs) in the presence of fetal bovine serum for 4-6 days and then plate the

EBs on gelatin coated tissue culture plates[7]. This will yield three-dimensional EBs with beating cardiomyocytes. In contrast, there is a protocol in which the cells do not go through a suspension phase but are instead co-cultured in the absence of serum with visceral endoderm like cells (END2) which secrete a still yet unknown factor which enhances cardiomyocyte differentiation[8]. And still another method is to take advantage of Activin-A and BMP4 signaling to induce cardiac differentiation, mimicking normal development but in a monolayer culture [7]. The differentiating cells and resulting cardiomyocytes express several molecular genetic markers we routinely use to validate them. Most commonly we examine transcription factors such as Gata4, Mef2, Nkx2.5 and also several cardiac specific structural proteins, including α/β -MHC, MLC-2V/2A and α -Actinin among others[5]. The independently beating areas have been characterized through their action potential profiles which show nodal-like, embryonic atrial-like and embryonic ventricular-like profiles[6].

MicroRNAs (miRs) are ~ 22 nucleotide, non-coding, single-stranded RNA molecules that lead to either translational repression or target degradation by either binding with imperfect or perfect homology, respectively, to the 3' UTR region of the target mRNA sequence[9]. A single miR is capable of targeting more than one gene and that genes are targeted by multiple miRs. The miR pathway takes advantage of the same machinery that is involved in siRNA biogenesis, namely the RISC-mi/siRNA complex which binds to the 3' UTR of the target sequence[10].

The first identified miRs, Lin-4 and Let-7 in *c. elegans*, were shown to be involved in gene regulatory networks that control larval developmental, but miRs

have also been shown to be involved in differentiation, proliferation, apoptosis and processes that depend upon spatiotemporal regulation of protein levels[11]. Currently, there are over 5000 miRs as reported in miRBase 10.0; of which 545 have been found in human models. Recently, there have been many studies utilizing in-vivo models that have led to the identification of novel miRs relevant to cardiac differentiation, stress-induced hypertrophy and heart failure [12-15]. Recent papers have shown that heart development and models of hypertrophy are regulated through miR expression in transgenic mice [13, 15-17].

An understanding of miRs is important to a thorough understanding of gene regulatory networks. Therefore pursuing the activity of miRs in hESC cardiogenesis might lead to novel means of controlling differentiation of cardiomyocytes, possibly by regulating the specific miRs themselves. The possibility that miRs regulate key steps in cardiogenesis led me to identify and characterize miRs that are differentially expressed as hESCDCs differentiate in vitro. Importantly I began experiments to devise over-expression and knock-down experiments for determining the function of miRs. These studies will focus on those that affect the incidence of differentiation or proliferation of isolated hESCDCs.

The Notch signaling pathway has been of great interest in cardiogenesis. The Notch receptor is a ~300 kd transmembrane protein that has four members in its class (Notch 1-4) that can bind the membrane bound ligands Delta 1, 3, 4 and Jagged/Serrate 1, 2. Upon the Notch receptor binding to one of its ligands, the intracellular domain (ICD) gets released and associates with the transcription factor RBPJ κ . The NICD:RBPJ κ complex then translocates to the nucleus where it

activates gene transcription [18]. Notch has been shown to be involved in the proliferation and differentiation of progenitor cells in different systems [19-24]. Furthermore, Notch is important for correct mouse heart development [19] and in humans, mutations in the Notch pathway lead to cardiac defects [25]. More importantly, it has been shown in a mouse ESC model that in the undifferentiated population there is a high activity of Notch signaling while it is reduced during cardiac cell differentiation [26].

Cardiomyocytes exit the cell cycle and stop dividing soon after birth as they mature [27-29]. Similarly, hESCDCs exit cell cycle and differentiate in culture and this currently prevents the expansion of the cardiomyocyte population to the amounts needed for therapeutic purposes. During fetal development, however, cardiomyocytes normally proliferate, indicating that some developmental signals sustain cell cycle as the number of muscle cells in the heart grows. Other experiments with the lab showed that Notch can sustain cell cycle of immature cardiomyocytes.

There are data supporting the interaction between Notch signaling and miR activity in other systems [30-32]; thus we explored the hypothesis that miRs might either regulate Notch activity or vice-versa in the developing cardiomyocyte. Specifically, I analyzed the miR expression profiles of NRVCs, which normally lack Notch signaling, to those in which we forced re-activation of Notch.

Chaper 1--MicroRNA Profiling of hESC Derived Cardiomyocytes

Abstract

Human embryonic stem cell derived cardiomyocytes (hESCDC) hold great promise for potential cell based therapy in which their derivatives could be utilized to repair a patient's infarcted heart. Many challenges remain before this type of treatment can be realized in the heart. These challenges include: increasing the incidence of the hESCs that differentiate into the cardiomyocyte lineage; inducing proliferation of the isolated hESCDC to levels needed for therapeutic purposes and also controlling maturation of the hESCDCs so that they can function comparably to the adult recipient ventricular myocardium. Here we used the hESC H9 line that had been modified so that purification of the cardiomyocyte lineage is possible through drug selection. With the purified cardiomyocyte populations we then undertook a miR microarray study to profile the miRs that change in expression as hESCs differentiate and at several different time-points of drug selected and isolated cardiomyocytes. Numerous miRs were found to vary during hESC and hESCDC differentiation.

Introduction

Several studies have analyzed miR profiles of differentiating hESC by various methods, such as through microarrays or through pcr analysis. miRs also have been shown to be involved in cardiac specific differentiation in many species [17, 32] as well as being involved in models of cardiac hypertrophy and heart failure [12, 13, 16, 33-35]. Our experiments analyzing the miR profile of hESCDCs in

hopes of finding novel miRs that contribute to the differentiation, proliferation and maturation of the cardiomyocyte pool.

Materials and Methods

hES Cell Culture and Differentiation

The hES line that was used for the following studies was the H9 from WiCell and was modified by infecting with a dual-cassette lentivirus vector to direct expression of Neomycin^r gene under the stem cell-specific promoter, Rex, and also Puromycin^r under the cardiomyocyte-specific α -MHC promoter (Figure 1A). The infected cells were selected with Neomycin and expanded. The cells were cultured in 6-well plates (Corning Inc.) in the presence of 80% Knock-Out DMEM (Invitrogen), 20% Knock-Out Serum Replacement (Invitrogen), 1% Non-essential amino acids, 1 mM L-Glutamine, 1% Antibiotic/antimycotic, 1 mM β -mercaptoethanol and 4 ng/ml bFGF (Sigma). The undifferentiated colonies were cultured on a monolayer of irradiated mouse embryonic fibroblasts and media was changed daily. The cultures were split 1:3 every 7 days by incubating the cells in 1 mg/ml Collagenase IV for ~5 min. or until rounding up of the colony edges was observed. The colonies were then detached using a 2 ml serological pipette, collected and transferred to new wells.

The differentiation media was identical except the knock-out serum replacement was replaced with 20 % FBS (Hyclone, Cat. # SH30070.03) and bFGF was excluded. One day before differentiation the culture was treated with 200 ng/ml Neomycin to selectively remove the mEFs. On the day of differentiation, and subsequent EB formation, the cultures were incubated with 1 mg/ml Collagenase IV

for ~5 min. or until rounding-up of the colonies was observed. The wells were then scraped with a 5 ml. Falcon pipette in the presence of differentiation media and the cells were collected and allowed to settle in 15 ml. Falcon tubes. Once settled the media was aspirated and fresh media was used to re-suspend the cell clusters and they were transferred to ultra-low attachment 6-well plates (Corning Inc.) at a 1:1 ratio. After 6 days in suspension the EBs were transferred to 0.1% gelatin coated 6-well plates and allowed to attach. Spontaneously beating areas were observed from day 7 on. On day 12 the α MHC-positive beating areas were selected by treating the cultures with ~1.6 ug/ml Puromycin for 2 days and resulting cell clusters were cultured until they were to be harvested (Figure 1B). At the various time-points, ~60 beating areas were isolated per biological replicate for miR analysis. We isolated cardiospheres at day 19, 29 and 40 day time-points and for a baseline comparison of EBs we also harvested and analyzed EBs at day 2, 8, 10 and 14. A representative image of a puromycin-selected and isolated cardiosphere is located in Fig. 1C.

miRNA Analysis

Total RNA was isolated from cells or tissues by Trizol extraction (Invitrogen,CA) Small RNAs were separated from total RNA via PureLink miRNA column based fractionation (Invitrogen, CA). 500 ng of the small RNA fraction was labeled for microarray analysis with the NCodeTM microRNA Labeling System (Invitrogen, CA) and subsequently hybridized on the NCodeTM Multi-Species miRNA Microarray V2 (Invitrogen, CA). The samples were labeled in both channels

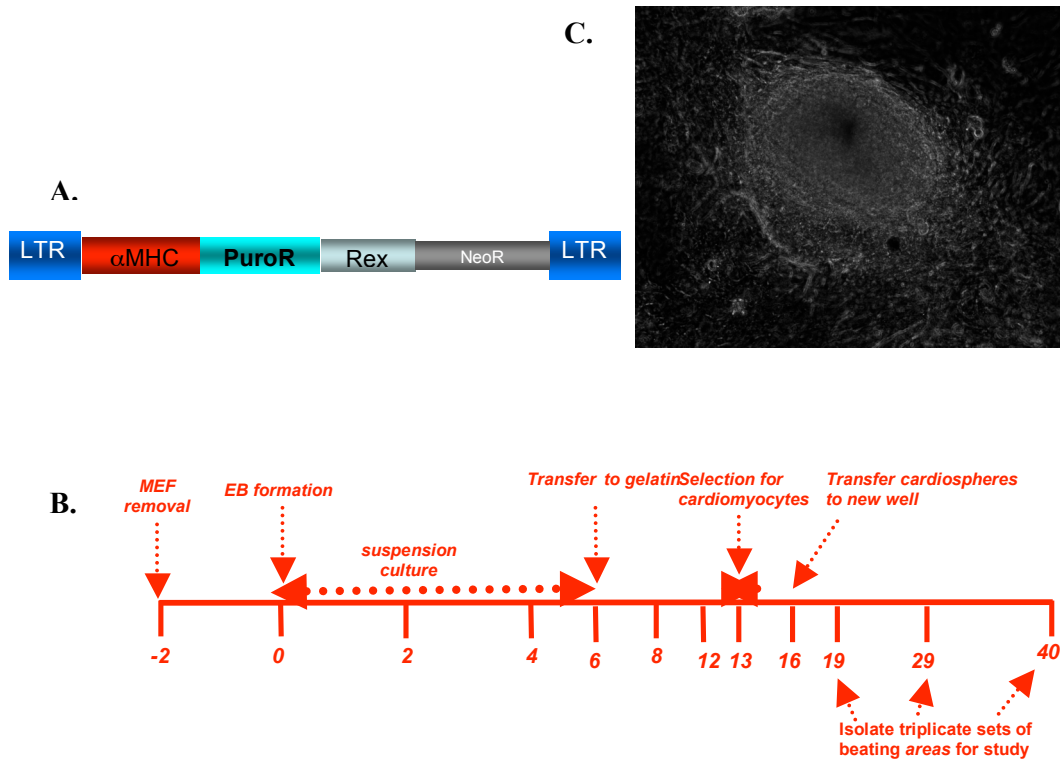
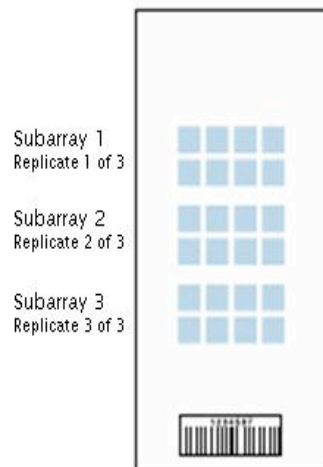


Figure 1: Representation of the lentiviral double-cassette used to infect the hESC H9 line showing puromycin resistance being driven by the cardiomyocyte specific α -MHC promoter and Neomycin resistance being driven by the undifferentiated marker Rex (A). Time-course depiction for the differentiation of the hESC H9 line to the cardiomyocyte lineage (B). Day 55 puromycin selected cardiosphere, brightfield image (C).



miRBase release 9.0 plus additional content

- Three replicate subarrays
- Hybridization controls
- Positive and negative controls
- Dye normalization controls

Probe content	Number of Probes
Human	553
Mouse	427
Rat	261
<i>C. elegans</i>	115
<i>D. melanogaster</i>	85
Zebrafish	371
Mismatch controls	76
NCode™ positive control	1 (72)*
NCode™ dye normalization controls	5
Small nucleolar RNAs	10
*The NCode™ Positive Control is spotted throughout the three subarrays	

Figure 2: Invitrogen representation of the microarray used for the microRNA expression studies.

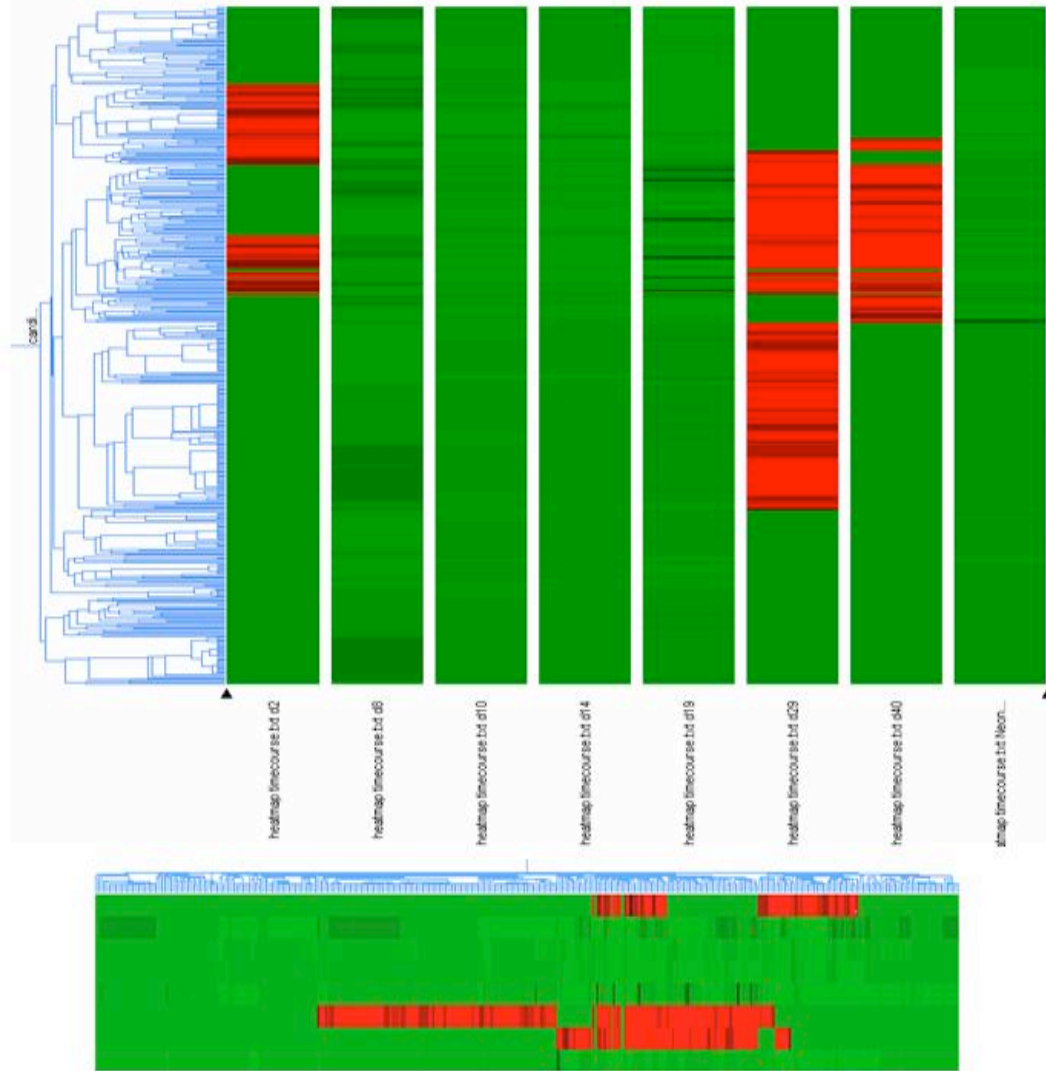


Figure 3: Representative heat-map showing global changes across various time-points of cardiomyocyte differentiation. Cardiomyocytes were isolated at day 19, 29 and 40. Embryoid bodies were harvested at day 2, 8, 10 and 14 of differentiation. Embryoid bodies contain multiple lineages in addition to cardiomyocytes

and were dye swapped and/or set-up in a loop model to account for variation associated with dye performance and chip to chip variability. The arrays were scanned using the Axon Scanner 4000B and data was acquired via GenePix 4.0 software. Data analysis was performed using NCode™ Profiler software. Data were background corrected, normalized via latin squares normalization. The fold change for each miR was calculated from undifferentiated H9's and filtered by statistical significance (parametric ANOVA p-value). A representative portion of the miR hits were analyzed by qRTPCR to validate the microarray results. GeneSpring software was used to create heat-maps for visualizing changes in global miR expression.

Results

In order to analyze the miR expression profiles of the hESCDCs, triplicate biological replicates were isolated after puromycin treatment that contained ~70 independently beating areas (cardiospheres). We analyzed d19, d29 and d40 time-points after drug selection and also included a d14 time-point prior to puromycin treatment which contained the beating cardiospheres in addition to the other lineages that arose during differentiation. We utilized the NCode microarray (Invitrogen) that contained all content from mirBase 9.0 in addition to positive and negative controls; and hybridization and dye normalization controls. First, a heat-map representing the global changes across each time-point (Fig. 3) indicates that the d29 and d40 time-points have significant changes in their miR profiles in relation to the undifferentiated population, as indicated by the orange areas.

We confirmed the presence of previously characterized cardiomyocyte specific miRs in the samples. These included miR-1 and miR-133, as shown in Table 1, that were highly enriched in the cardiomyocyte samples. In addition, we confirmed that pluripotency related miRs, or those that are involved in maintaining the undifferentiated state, were decreased. For example, the miR-302 family (miR-302a, b, c and d) was significantly decreased in relation to the undifferentiated population (Table 1).

We identified changes in miR expression during cardiomyocyte differentiation. Chart 1 shows that miR-1 increases significantly as differentiation proceeds. This trend is in line with what we would expect, since in previous studies miR-1 has been shown to target the transcription factor Hand2, which has been shown to promote the expansion of ventricular cardiomyocytes during the process of differentiation [17] and also miR-1 targets HDAC4 which acts as a transcriptional repressor and is involved in muscle gene expression [36]. From our studies, the miR-1 level is low at day 19 of differentiation, when the hESCDCs are still proliferative consistent with a role for miR-1 in promoting terminal differentiation. At day 40, in contrast, miR-1 levels are high which would correspond to terminal differentiation and therefore an exit from the cell-cycle.

An inverse trend was seen with miR-133, which has been shown to target serum response factor (SRF) [9] during cardiac and skeletal muscle development in addition to being involved in mouse models of cardiac hypertrophy [33]. With this known, and that at the day 19 & day 29 time points miR-133 expression coincides closely with miR-1 expression, which is also when the hESCDCs are still known to

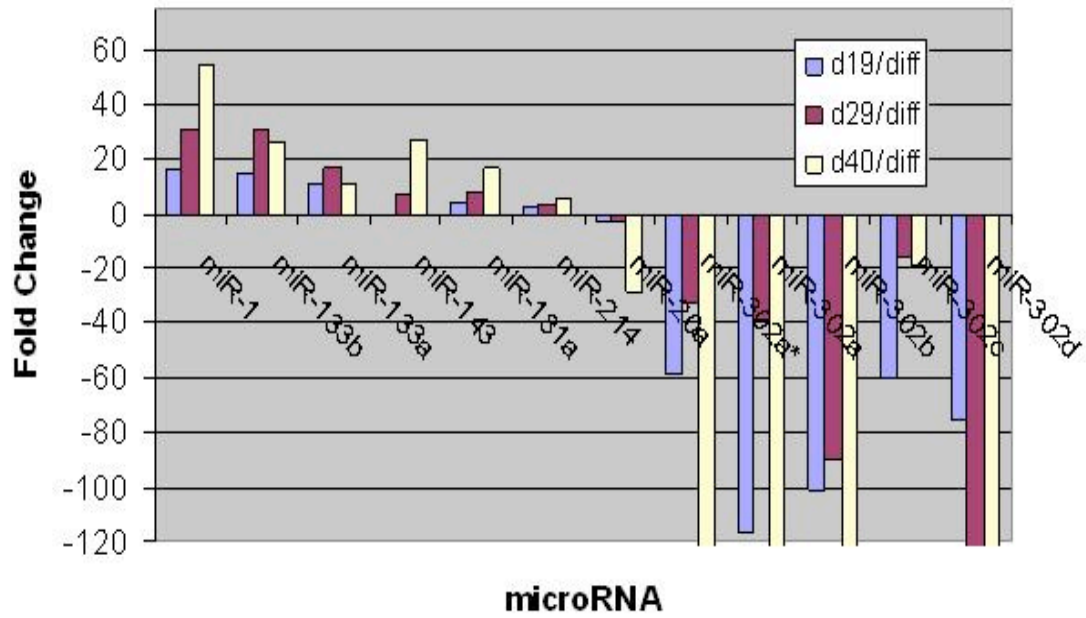
Table 1: Upregulated miRs relative to undifferentiated hESC H9. miRs in red have been shown to be expressed in adult mouse heart. Where the fold change is in red, this denotes that the miR has changed significantly in mouse models of cardiac hypertrophy in response to trans-aortic constriction.

Upregulated microRNA									
Day 14		Day 19				Day 29		Day 40	
miR	Fold Δ	miR	Fold Δ	miR	Fold Δ	miR	Fold Δ	miR	Fold Δ
497	5.5	122a	32.7	328	2.3	1	30.8	1	54.3
		1	15.7	532	2.3	133b	30.3	143	27.1
		133b	14.9	575	2.3	133a	16.5	133b	26.1
		483	12.3	346	2.3	181a	8.0	181a	17.2
		181b	10.7	149	2.3	143	7.8	30d	16.6
		133a	10.5	451	2.3	181b	6.4	27b	13.9
		126	9.8	99a	2.3	483	5.2	133a	10.8
		595	5.4	199b	2.3	151	5.0	210	9.7
		218	5.2	628	2.2	301	4.2	let7e	8.5
		198	4.9	656	2.2	100	3.9	24	8.3
		145	4.4	660	2.2	219	3.8	let7a	8.3
		181a	4.3	208	2.2	181c	3.6	422b	7.0
		152	4.1	630	2.2	500	3.4	23b	7.0
		215	4.0	449b	2.2	660	3.3	9'	6.9
		513	3.9	146b	2.2	145	3.3	199a'	6.5
		10b	3.8	214	2.2	199b	3.3	214	5.6
		499	3.8	453	2.1	210	3.2	125b	5.2
		574	3.6	338	2.1	499	3.2	30b	5.1
		10a	3.6	219	2.1	125a	3.1	26a	4.2
		194	3.4	4853p	2.0	122a	3.1		
		223	3.3	642	2.0	214	3.0		
		192	3.3	202	2.0	491	3.0		
		100	3.3	147	2.0	362	2.8		
		615	3.1	193a	2.0	152	2.7		
		320	3.0	490	2.0	205	2.7		
		370	2.8	383	2.0	30a3p	2.7		
		206	2.8	501	2.0	22	2.6		
		197	2.7	217	2.0	181d	2.6		
		30a3p	2.6	5425p	1.9	203	2.6		
		432	2.6	3243p	1.9	130b	2.5		
		584	2.5			584	2.5		
		181d	2.5			27b	2.5		
		449	2.4						
		627	2.4						

Table 2: Downregulated miRs relative to undifferentiated hESC H9. miRs in red have been shown to be expressed in adult mouse heart. Where the fold change is in red, this denotes that the miR has changed significantly in mouse models of cardiac hypertrophy in response to trans-aortic constriction.

Downregulated microRNA											
Day 14		Day 19						Day 29		Day 40	
miR	Fold Δ	miR	Fold Δ	miR	Fold Δ	miR	Fold Δ	miR	Fold Δ	miR	Fold Δ
214	-2.7	30b	-2.0	222	-3.2	519b	-5.0	518f*	-2.5	372	-10.8
23a	-2.7	36f	-2.0	374	-3.2	489	-5.1	20a	-2.6	517a/b	-12.6
9*	-2.9	98	-2.0	204	-3.2	520a*	-5.1	18a	-2.6	373	-17.3
18b	-2.9	577	-2.1	26a	-3.2	379	-5.1	18b	-2.6	302c	-19.0
22	-3.0	526c	-2.1	175p	-3.3	30c	-5.2	19a	-2.6	20a	-28.4
25	-3.1	9*	-2.1	14f	-3.3	2f	-5.3	519c	-2.6	302b	-210.4
23b	-3.1	518c*	-2.1	92b	-3.3	93	-5.3	526c	-2.7	302a	-212.1
181b	-3.1	598	-2.2	199a	-3.3	let7c	-5.4	522	-2.8	302a*	-250.6
199a*	-3.1	200a	-2.2	4255p	-3.3	let7g	-5.6	let7d	-2.8	302d	-334.9
19a	-3.2	let7b	-2.2	106b	-3.4	422a	-5.8	183	-2.8		
18a	-3.2	103	-2.3	106a	-3.4	let7d	-6.1	494	-2.8		
99b	-3.3	27a	-2.3	128b	-3.4	526b	-6.5	5123p	-2.9		
15b	-3.5	42f	-2.3	520b	-3.4	363	-7.1	374	-2.9		
36f	-3.6	2995p	-2.3	28	-3.6	7	-7.3	195	-3.0		
125b	-3.6	519a	-2.3	524*	-3.6	422b	-7.3	128b	-3.0		
130b	-3.8	185	-2.4	565	-3.7	127	-7.4	146a	-3.1		
107	-3.9	15a	-2.4	34a	-3.7	519c	-8.1	519d	-3.1		
103	-3.9	590	-2.4	128a	-3.8	15b	-8.3	524'	-3.5		
30c	-3.9	22f	-2.5	518b	-3.9	517c	-8.6	367	-3.7		
19b	-3.9	365	-2.5	526a	-3.9	let7a	-9.1	15b	-3.8		
10a	-3.9	522	-2.5	124a	-4.0	18a	-9.8	let7f	-3.9		
27b	-3.9	19f	-2.5	20b	-4.0	520g	-9.8	5165p	-3.9		
16	-4.0	520d	-2.6	146a	-4.2	18b	-10.0	37f	-4.1		
26a	-4.1	107	-2.7	29b	-4.3	367	-10.7	148a	-4.2		
30b	-4.2	19b	-2.7	200b	-4.3	182	-10.8	5153p	-4.2		
125a	-4.2	155	-2.7	25	-4.3	5165p	-11.4	7	-4.2		
92	-4.2	34c	-2.7	173p	-4.4	200c	-11.9	182	-4.3		
130a	-4.3	20a	-2.8	520h	-4.4	let7f	-11.9	526a	-4.6		
19f	-4.3	92	-2.8	5153p	-4.4	519d	-12.0	let7i	-4.8		
106b	-4.3	498	-2.9	525	-4.5	3f	-12.2	489	-5.5		
24	-4.4	19a	-2.9	10f	-4.8	29a	-15.2	372	-6.4		
122a	-4.6	148a	-3.1	195	-4.8	520c/f	-15.3	302c'	-7.7		
320	-4.7	125b	-3.2	183	-4.9	187	-18.2	373	-8.5		
30a5p	-4.9	16	-3.2	518f*	-4.9	37f	-18.5	187	-12.3		
143	-4.9					5123p	-19.4	302c	-15.5		
20a	-5.2					372	-22.6	302a'	-32.9		
181a	-5.4					let7f	-26.6	302a	-38.4		
126	-5.8					302c*	-39.9	302b	-90.0		
93	-6.0					373	-43.5	517a/b	-93.3		
30d	-6.3					373	-46.8	302d	-122.0		
335	-7.2					302a*	-58.5				
						302c	-60.0				
						517a/b	-63.5				
						302d	-75.5				
						302b	-100.9				
						302a	-116.6				

Graph 1: Histogram comparing expression of common miRs between day 19, 29 and 40 in selected and isolated cardiomyocyte populations relative to undifferentiated hESCs. All fold change values were statistically significant ($p < 0.05$).



be in a proliferative state. At day 40 however, miR-133 expression decreases slightly while miR-1 continues to rise. This would support the conclusion that an increase in miR-1 and decrease in miR-133 would diminish the proliferative capacity of the hESCDCs, consistent with previous reports [36].

We have begun to compare the miR expression profile against those miRs known to be expressed in cardiac tissue. Table 1 shows the enriched population of miRs in hESCDCs, the miRs in red have been shown to be elevated in adult mouse heart [12]. This suggests that the developing hESCDCs are acquiring a miR profile similar to that of adult cardiac tissue. Table 2 lists the population of miRs that have decreased during differentiation towards the cardiomyocyte lineage, e.g. were enriched in the undifferentiated state. Note that a number of miRs, those in red, have also been shown to be enriched in adult mouse cardiac tissue but were more enriched in the undifferentiated population than in the hESCDCs. From this result we conclude that the hESCDC profile remains dissimilar from the adult cardiac tissue. Moreover, several miRs previously shown to be enriched in adult mouse heart [12] were not detected, or were not characterized as statistically significant, in the hESCDCs.

Discussion

Our analysis of the miR expression profile of the hESCDCs at various time-points of differentiation is the first step to determine functional targets for miRs that are involved in the differentiation, proliferation and maturation of the hESCDCs. We are currently determining those genes that are expressed in the hESCDCs and

undifferentiated hESCs using the Affymetrix GeneChip® Human Exon 1.0 ST Array in collaboration with Bruce Conklin's Lab at UCSF. Moreover, since it is an exon array it will provide us with more information regarding potential targets for specific miRs giving us information on the proteins being expressed.

We also plan to utilize Invitrogen's SILAC labeling system to prepare samples for mass spectrometry analysis of age matched samples to determine the protein translational profile for both undifferentiated ESCs and the hESCDCs. Together with the data from the Human Exon array these data will permit us to develop testable hypothesis about specific expression. We will then undertake functional studies that will include utilizing in-vivo models of either conditional knock-outs or over-expression models to confirm more concretely the actual targets of specific miRs.

Chaper 2--MicroRNA Analysis of Notch Activated Neonatal Rat Ventricular Cardiomyocytes

Abstract

NOTCH2 is expressed in the developing myocardium but its levels decrease after birth when terminal differentiation and maturation occur. Shortly after birth Neonatal Rat Ventricular Cardiomyocytes (NRVCs) exit the cell cycle and become quiescent, and this correlates with a decrease in Notch signaling activity. Sustaining Notch signaling causes ESC-derived cardiomyocytes and NRVCs to continue dividing and thus might be important to control expression of the pool of cardiomyocytes during fetal development. Here we studied whether miRs might influence Notch pathway activation and cell cycle entry.

Introduction

In mammalian systems, cardiomyocytes exit the cell cycle and stop dividing soon after birth when cardiomyocytes are in the process of maturing [27-29]. In the case of hESDCs, cell cycle exit and differentiation prevents the expansion of the cardiomyocyte population to the amounts needed for therapeutic purposes. Thus, we are interested in understanding signals that controls cardiomyocyte cell proliferation. This knowledge could lead to strategies to increase the number of mature cardiomyocytes for cell-based therapies.

Our lab has been focusing on the control of cardiomyocyte cell cycle by the Notch pathway. Notch has been shown to be involved in the proliferation and differentiation of progenitor cells in different systems [19-24]. Furthermore, Notch is

important for correct mouse heart development [19] and in humans, mutations in the Notch pathway lead to cardiac defects [25]. More important, it has been shown in a mouse ESC model that in the undifferentiated population there is a high activity of Notch signaling while it is reduced during cardiac cell differentiation [26]. Recently, our lab has shown that Notch sustains cardiomyocyte cell cycle entry leading to proliferation of immature cardiomyocytes (Campa, et al, 2007, submitted). We hypothesized that miRs might be involved in Notch mediated control of cell cycle.

miRs are able to regulate gene expression through their binding to a mRNA's 3' UTR and inhibiting its translation. Recent papers have shown that heart development and models of hypertrophy are regulated through miR expression in transgenic mice [13, 15-17]. Also, there are data supporting the interaction between Notch signaling and miR activity in other systems [30-32]. Specifically, we wanted to test the idea that miRs might work as mediators or feedback inhibitors of Notch mediated cell cycle entry. Therefore, we analyzed the miR expression profiles of NRVCs that have their Notch pathway activated in comparison to untreated NRVCs which have very low or no Notch signaling.

Materials and Methods

Neonatal rat ventricular myocyte isolation and culture

Wild-type NRVCs were isolated from 1-2 day old wild-type rats using the Cardiomyocyte Isolation Kit (Cellutron Life Tech.). Cells were plated for 24 hrs in media containing 10 % Horse serum, 5 % FBS, 84 % DMEM:F12, 1% Antibiotic/Antimycotic, 100 μ m Ascorbic acid, 3 mM Sodium Pyruvate, 4 μ g/ml Transferrin and 2 g/l BSA. After 24 h a portion of the cells were switched to the above media but containing only 0.25 % FBS and the rest were continued in high serum. Seventy-two hours after isolation the cells in 0.25 % FBS were infected for 12 hours with either adenovirus expressing the intra-cellular domain of Notch2 (Ad-N₂ICD, Gift of Tom Maciag) or an adenovirus expressing β -galactosidase (Ad- β -Gal, Clontech) as a control. After 24 hours of infection the cells were frozen at -80 in Trizol.

In addition, the full length cDNA for hJagged1, which is one of the membrane bound ligands for the Notch receptor, was cloned into pADTrack-CMV-GFP (Stratagene), linearized to reveal the right and left ITR's and subsequently transfected into HEK-293s to produce the virus. The virus producing cells were collected, lysed through repeated freeze-thaw cycles, and the filtered. The resultant viral supernatant was then used to infect a monolayer of irradiated neonatal rat cardiac fibroblasts and these hJagged1 expressing fibroblasts were used to induce Notch signal in cardiomyocytes.

miRNA isolation and microarray analysis

Total RNA was isolated from cells or tissues by Trizol extraction (Invitrogen,CA). Small RNAs (<200 nt) were separated from total RNA via PureLink miRNA column based fractionation (Invitrogen, CA). 500 ng of the small RNA fraction was labeled for microarray analysis with the NCode™ microRNA Labeling System (Invitrogen, CA) and subsequently hybridized on the NCode™ Multi-Species miRNA Microarray V2 (Invitrogen, CA). The samples were labeled in both channels and were dye swapped and/or set-up in a loop model to account for variation associated with dye performance and chip to chip variability. The arrays were scanned using the Axon Scanner 4000B. Data was acquired via GenePix 4.0 software. Data analysis was performed using NCode™ Profiler software. Data were background corrected, normalized via latin squares normalization. The fold change was calculated from NRVCs infected with Adeno-β-gal and filtered by statistical significance (parametric ANOVA p-value). A representative portion of the miR hits were analyzed by qRTPCR to validate the microarray results. GeneSpring software was used to create heat-maps for visualizing changes in global miR expression.

Results

Activation of the Notch pathway

In order to study the effects that the Notch pathway has on miR expression and cell-cycle entry we devised a way to activate the Notch pathway through over-expression. This was accomplished was through the use of an adeno-virus expressing

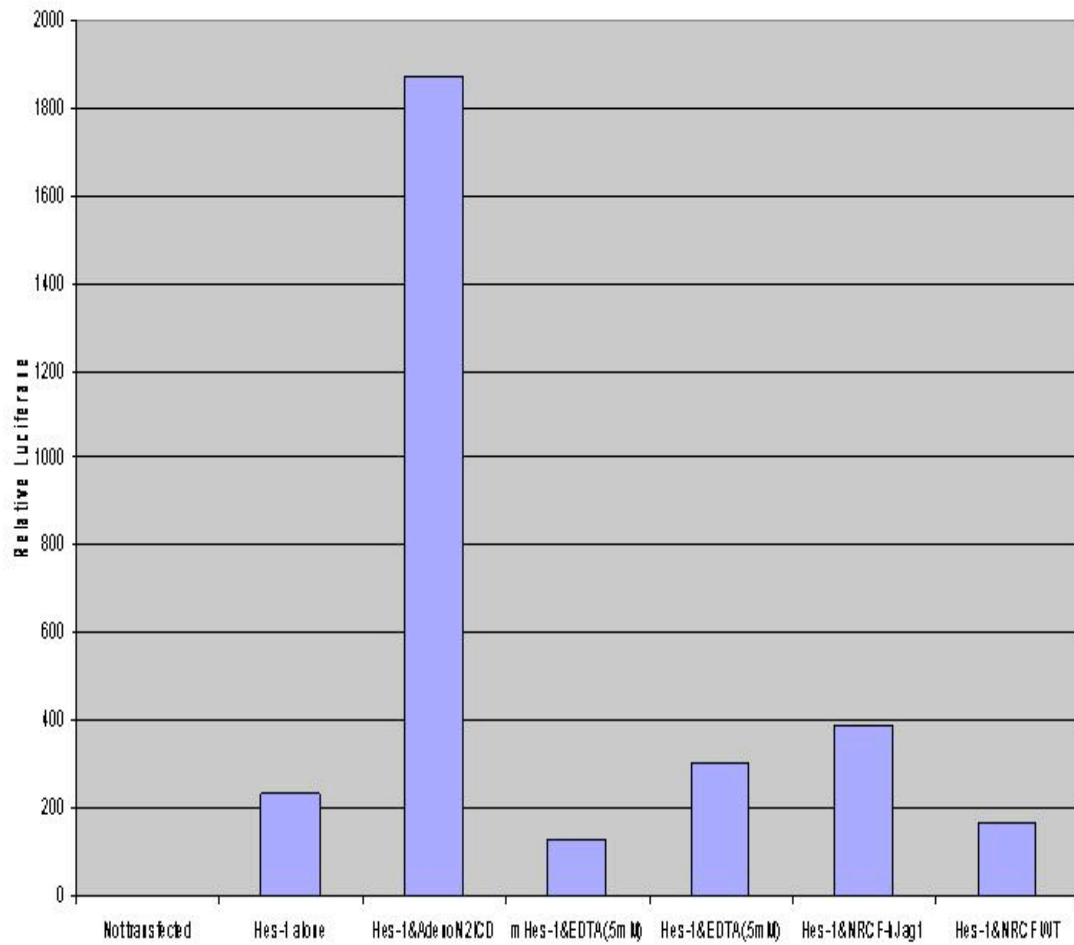


Figure 4: Activity of recombinant hJagged1 on surface of Ad-hJagged1 infected NRCFs. Infected NRCFs were co-cultured with Hes-1 luciferase or mutant Hes-1 luciferase in transfected HeLa cells and luciferase activity was plotted relative to Ad-N2ICD-infected HeLa cells as a positive control

the intra-cellular domain of Notch2 (Ad-N₂ICD). The function of the Ad-N₂ICD was detected through use of a luciferase reporter under regulation of the Hes-1 promoter which is a downstream target of Notch2. Figure 4 shows that when HeLa cells that were transiently transfected with Hes-1 luciferase and then were infected with Ad-N₂ICD the luciferase value was 9-fold greater than in the sample with Hes-1 luciferase alone without Notch activation.

To obtain a relatively more physiological increase in Notch signaling we stimulated endogenous Notch receptors using hJagged1 on a feeder layer of cardiac fibroblasts infected with an adenovirus vector directing expression of hJagged1. First, Neonatal Rat Cardiac Fibroblasts (NRCFs) were infected with Ad-hJagged1-GFP and subsequently stained with anti-hJagged1 antibodies to confirm the production of hJagged1 protein as shown in Fig. 5. HeLa cells, which endogenously express the Notch2 receptor, as shown in Fig. 6, were transfected with Hes-1 luciferase or a mutated form of Hes-1 luciferase that was unable to respond to Notch as a control and plated on a monolayer of the hJagged1 infected NRCFs. The relative luciferase values were determined and as is shown in Figure 4 the cells that were plated on the hJagged1 expressing cells had a 2-fold increase in Notch signaling above the control cells without the hJagged1 ligand present. Also, for comparison, the HeLa cells were treated with EDTA, a divalent cation chelator which leads to activation of the Notch pathway through disruption of the Notch extracellular-transmembrane domain and subsequent nuclear localization of the Notch intracellular domain [37] and as expected we saw an increase in Hes-1 luciferase

activity above the Hes-1 luciferase alone as shown in Fig. 4. Thus both Notch₂ICD and hJagged1 can be used to activate Notch signaling.

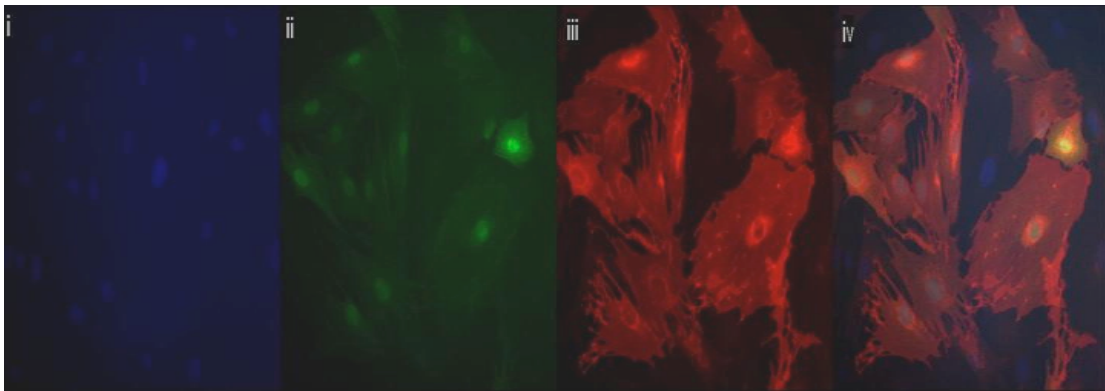


Figure 5: Neonatal Rat Cardiac Fibroblasts infected with Ad-GFP-hJagged1. Stained 48 hours after infection. (i) DAPI; (ii) eGFP; (iii) anti-hJagged1; (iv) Merge

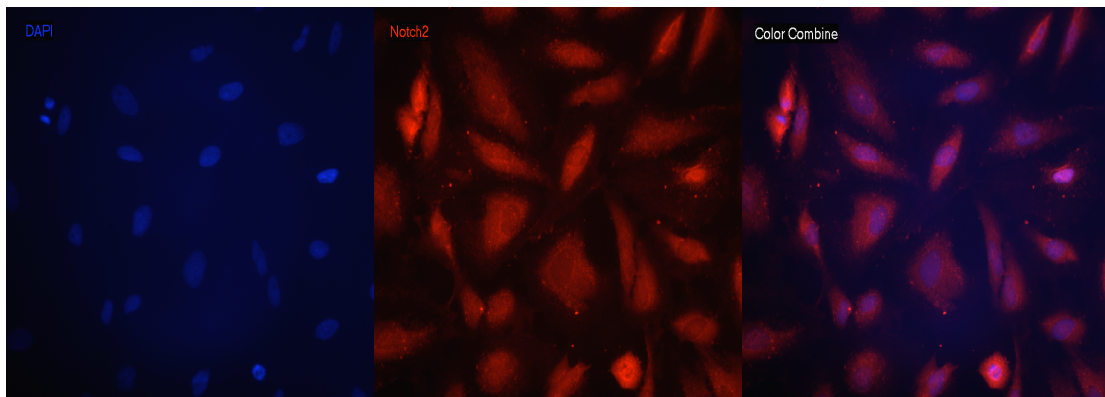


Figure 6: HeLa cells stained for Notch 2 (i) DAPI; (II) anti-Notch2; (iii) Merge

miRNA Expression Profiles of NRVCs infected with Ad-N₂ICD

Once we verified that it is possible to activate the Notch pathway through the previously described techniques, we wanted to determine the effect of Notch activation on miR expression. Using the V2 microRNA microarray described previously we compared the miR expression profile of the NRVCs infected with Ad-N₂ICD in comparison to the Ad-β-gal control. First, as a general representation, the volcano plot in Graph 1 shows the fold change versus p-value that is in response to Notch activation.

First we examined if cardiac specific miRs that are well known from the literature were present and detectable in our samples. As shown in Table 3 several muscle specific miRs such as miR-1 and miR-133 were enriched in these samples as expected [17, 36]. We then focused attention on those miRs that changed concordantly with Notch signaling and were deemed statistically significant. From the data presented in Table 3 we show that 47 miRs showed statistically significant variation ($P < 0.05$). Of the 29 miRs that were upregulated in response to Notch activation several had been shown by others to be cardiac specific. For example, miR-1 was 4-fold upregulated. Also, miR-1 has been shown to target the transcription factor Hand2 and histone deacetylase 4 (HDAC4) in mammalian systems and is responsible for cardiac muscle differentiation also targets the Notch ligand, Delta, in *Drosophila* (dmiR-1) [17, 32].

Graph 2: Significant change in miR expression with Ad N₂ICD. The following volcano plot represents the change in miR expression associated with Notch 2 expression. X axis represents fold change while y-axis represents statistical significance. miR expression data from AdNotch2 infected NRVCs were compared to data from Ad-β-gal infected NRVCs for significant change in expression. Data were background corrected normalized across entire experiment (Latin squares normalization). Fold change in miR expression was measured for each feature, statistical significance determined by students T-test and p-values assigned.

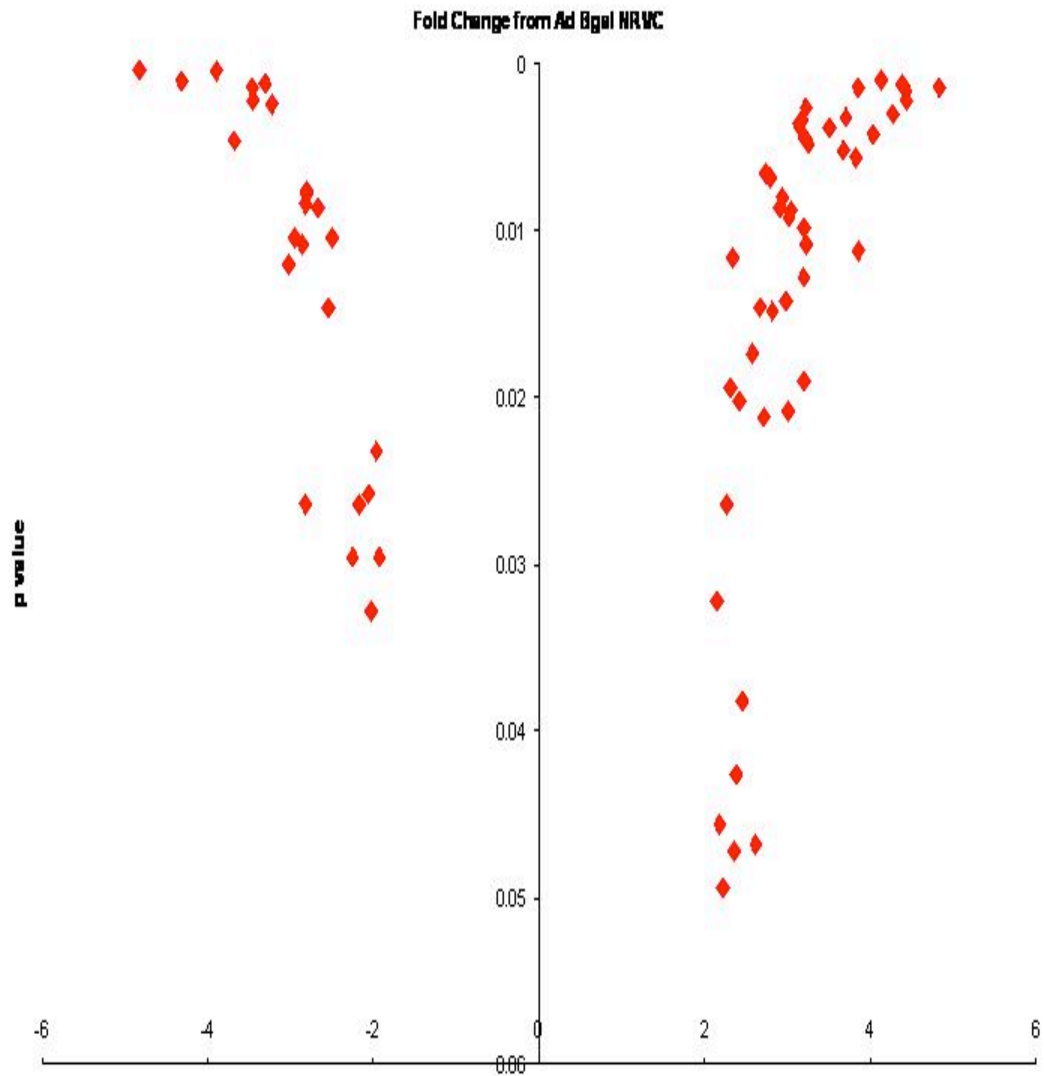


Table 3: Fold change in miR expression relative to undifferentiated hESCs. Significance was determined by Students T-test ($p < 0.05$). miR's in red have been shown to be expressed in adult mouse heart. Where the fold change is in red, this denotes that the miR has changed significantly in mouse models of cardiac hypertrophy in response to trans-aortic constriction.

Ad-Notch vs. Ad-β-gal			
Upregulated		Downregulated	
miR	Fold Δ	miR	Fold Δ
24	4.4	181a	-1.9
l7d*	4.4	125a	-2.0
320	4.3	181b	-2.0
130a	4.1	107	-2.1
133b	4.0	26a	-2.2
1	4.0	28	-2.3
297	3.9	151*	-2.5
103	3.8	422b	-2.7
l7c	3.8	23b	-2.7
l7e	3.8	l7d	-2.8
133a	3.7	25	-2.8
22	3.5	152	-2.8
143	3.2	29a	-2.8
499	3.2	344	-3.0
374	3.2	191	-3.2
l7b	3.2	99a	-3.3
346	3.2	15b	-3.5
16	3.0	30d	-3.5
361	3.0	20a	-3.7
185	3.0	214	-3.9
130b	3.0	335	-4.3
31	3.0	424	-4.8
26b	2.9		
92	2.8		
27a	2.7		
374	2.7		
30b	2.7		
17	2.7		
146	2.7		
298	2.6		
106b	2.5		
23a	2.4		
351	2.4		
125b	2.4		
221	2.3		
301	2.3		
l7i	2.2		
324-5p	2.2		
19b	2.0		

In addition, miR-133 which targets serum response factor was also upregulated in the Notch sample and had been shown to be involved in cellular proliferation [36]. Also, at the top of the list of upregulated miRs was miR-24 which was over 4-fold upregulated and it has been shown to be elevated in mouse models of cardiac hypertrophy. In contrast, miR-214 which was shown to be significantly upregulated during cardiac hypertrophy was down-regulated in response to Notch. Also, miR-125b which has been shown to be involved in cellular proliferation was upregulated in the Notch treated sample [11, 13]. It is important to emphasize that the fold difference values were calculated relative to an untreated population. In certain cases, the miR expression was not detected in the cells; thus, the fold difference was quite large. In such cases, we conclude that the miR was regulated by Notch but the magnitude of regulation is uncertain.

Discussion

Our experiments focused on the discovery of new miR targets of Notch signaling. Since Notch is important for cardiac development we hope that the modulation of miRs that are Notch-related might provide insight into Notch function and potentially provide a new tool to control cardiac proliferation and differentiation.

Based on our results, several miRs warrant further study as direct targets of Notch signaling. For example, miR-221, which was upregulated significantly has been shown to target the cyclin dependant kinase inhibitor (CDKI) p27^{Kip1} [38]. Interestingly, CDKI p27^{Kip1} knockout mice present cardiomyocyte hyperplasia [39]. We know from previous work in our laboratory that Notch2 over-expression leads to

cell cycle entry, as shown through KI-67 staining, even though they do not fully complete the cycle. Based on these data, we can propose the following model: over-expression of Notch2 leads to an increase in miR-221 expression which then targets the transcript for p27^{Kip1}. This decrease in the CDKI level would then contribute to cell cycle activation. Further studies are needed to validate that the correct target for miR-221 under these assay conditions is in fact p27^{Kip1}. This will be shown through the over-expression of miR-221 and the predicted outcome would be a decrease in the amount of p27^{Kip1}. Conversely, the recovery of p27^{Kip1} protein levels will be shown through an anti-sense miR-221 to knock-down the endogenous miR.

Another interesting miR downstream of Notch signaling is miR-107 which has been shown to target the transcript for Hypoxia inducible factor-1 α (HIF-1 α) [40]. HIF-1 α is part of a heterodimer with HIF-1 β and under low O₂ conditions HIF-1 α gets stabilized and leads to regulation of gene transcription. It has been described that an increase in HIF-1 α , induced by either hypoxic conditions or through regulators of HIF-1 α translation such as miRs, leads to an increase in vascular endothelial growth factor (VEGF) [41]. Unpublished work from our lab indicates that Notch is required for the hypoxic response in cardiomyocytes in response to ischemic stress caused by chronic hypertension in a transgenic animal model (Ramon Diaz Trelles, unpublished). Moreover, RBPJ κ , which mediates Notch dependant transcription, forms a complex with Hif-1 α . [42]. Our finding that Notch over-expression causes a down-regulation of miR-107 expression might indicate that the decrease in miR-107 expression would lead either to an increase, or at least prevent a

decrease in HIF-1 α levels. This stable or possibly elevated level of HIF-1 α in response to Notch would then contribute to an increase in expression of VEGF.

Potentially relevant for VEGF regulation by Notch, miRs -15b, 16, 20a and 20b each target VEGF, and their subsequent down-regulation leads to an increase in VEGF expression [41]. Of these, our data show that miR-15b and 20a levels are decreased significantly, which is consistent with the decrease in miR-107, and therefore supports a role in the increase of VEGF levels. Another miR, miR-16 which also has been shown to target VEGF, is upregulated in response to Notch activation. This might indicate either another target or, more interestingly, feedback regulation for VEGF.

Finally, an example of miRs modulating the Notch pathway is miR-15b which has been shown to target the F-box protein, FBW7. FBW7 is a ubiquitin ligase responsible for targeting cyclin E and the Notch receptor for degradation by the proteasome. Previous studies have shown that knock-down of FBW7 in transgenic mice causes an elevation in both cyclin E and also Notch signaling [43]. We observed that miR-15b was downregulated in response to Notch activation, suggesting that Notch activation, might negatively feedback via the decrease in miR-15b levels and would then lead to increase FBW7 levels. Elevated level of FBW7 would then trigger degradation of Notch. Verification of such a feedback loop awaits over-expression miR-15b while the Notch signaling pathway is also active, thereby showing 1) A decreased level of FBW7 and 2) prolonged elevation in Notch signaling. Conversely, depletion of miR-15b, through use of a complementary miR sequence would be expected to have the opposite effect. These examples illustrate a

few of the miRs that should be analyzed. Since the number of Notch-regulated miRs is large, we have begun to develop functional tests to use as secondary screens to identify those miRs that act as agonists or antagonists of Notch in NRVCs.

Chapter 3--Optimization of an High-Throughput Method of Transfection to Introduce Synthetic MicroRNAs into Neonatal Rat Ventricular Cardiomyocytes

Abstract

The previous chapter described experiments that identified numerous candidate miRs that might influence Notch signaling, both positively and negatively. Here I describe the development of function-based secondary screens to confirm activity of the miRs with tow effects of Notch: cell cycle entry and VEGF gene expression. These assays will be used to screen through the 61 miRs regulated by Notch and the corresponding complementary miRs to test biological activity.

Introduction

The goal of these experiments is to optimize a high-throughput procedure to introduce and quantitate the effect that specific miRs have on Notch regulation of cell cycle and VEGF induction. We chose to use a reverse-transfection method in which the oligos and transfection reagent are plated on the bottom of the 384-well dishes based upon the potential scalability of cationic/liposome based delivery to a high-throughput format.

Materials and Methods

Neonatal Rat Ventricular Cardiomyocyte Isolation and Culture

The neonatal cells were isolated as described in Chapter 3. Cells were cultured in high serum media, as previously described, for 24 hours after isolation. They were then switched to media containing only 0.25% FBS for another 48 hours. At this time the cells were detached using 0.25 % Trypsin for 5 min., counted, and 3×10^3 ventricular cardiomyocytes per well were plated on 1% gelatin coated 384-well plates in the low serum media.

Transfection of Ventricular Cardiomyocytes or Cardiac Fibroblasts

The wells upon which the cells were plated contained one of the following transfection reagents at manufacture recommended amounts: Dharmafect 1, 2, 3, 4 (Dharmacon); X-treameGENE (Roche); Lipofectamine 2000 (Invitrogen); Lipofectamine RNAi Max (Invitrogen); TransIT TKO (Mirus); TransIT siQuest (Mirus) or HiPerFect (Qiagen). The transfections were performed in triplicate with 0.5 μ M of the following: a siRNA to GAPDH; an unspecific siRNA or a no siRNA control. Briefly, prior to plating of the cells, 1 μ l of the siRNA was spotted on the appropriate wells; 0.1 μ l of each transfection reagent, (0.5 μ l for HiPerFect), was mixed with 10 μ l Opti-Mem I and added to the corresponding well; the wells were incubated at room temperature for 20 minutes and 40 μ l of the cell suspension was added to each well for a total of \sim 50 μ l. The transfection was performed for 72 hrs. after which time the wells were washed in 1x PBS, fixed in 4% paraformaldehyde and stained for GAPDH, α -actinin and DAPI to identify the cardiomyocyte

population and to determine the knock-down potential for each reagent. Also, the amount of cells before and after the transfection was counted to determine the toxicity of the individual reagents.

Results

Transfectability of Neonatal Rat Ventricular Cardiomyocytes (NRVCs)

After transfecting 3×10^3 ventricular cardiomyocytes in the 384-well format with the panel of transfection reagents, we determined DharmaFECT3 produced the best target knock-down and had the lowest toxicity in comparison to the other reagents tested (Fig.7, 9). Lipofectamine 2000 was one of the more toxic reagents and it did not transfect NRVCs well based upon the levels of GAPDH expression (Fig.8).

The knock-down was determined through transfection of a siRNA specific to endogenous GAPDH and the cells were subsequently stained with a rabbit polyclonal antibody to GAPDH (AbCam, ab9485). The cells were also counter stained to identify the cardiac population with a monoclonal mouse antibody to α -actinin (Sigma). The average fluorescent signal per well was then calculated to determine the percentage knock-down. Also, the toxicity of the individual reagent was then determined by counting the cell number per well before and after transfection with the assumption that the dead cells would detach and therefore be removed during the washing steps.

High-throughput Method of Transfection and Quantitation

In order to utilize this transfection on a larger scale we took advantage of automated technologies in order to alleviate repetitive manual pipetting and other laborious processes. After isolation of the cardiomyocytes we utilized the Matrix Wellmate to plate 3×10^3 cells per well in a 384-well format for the plates which contained the transfection reagents and siRNA. After the transfection, the plates were then processed on the Titertek Map-C which performed all of the immunofluorescence staining procedure. For quantitation, the processed plates were then scanned and the relative fluorescence intensities were determined per well. This automated process, which allowed minimal manual handling of the samples, greatly increased the number of potential compounds/reagents that can be tested, while significantly reducing the time and cost of processing.

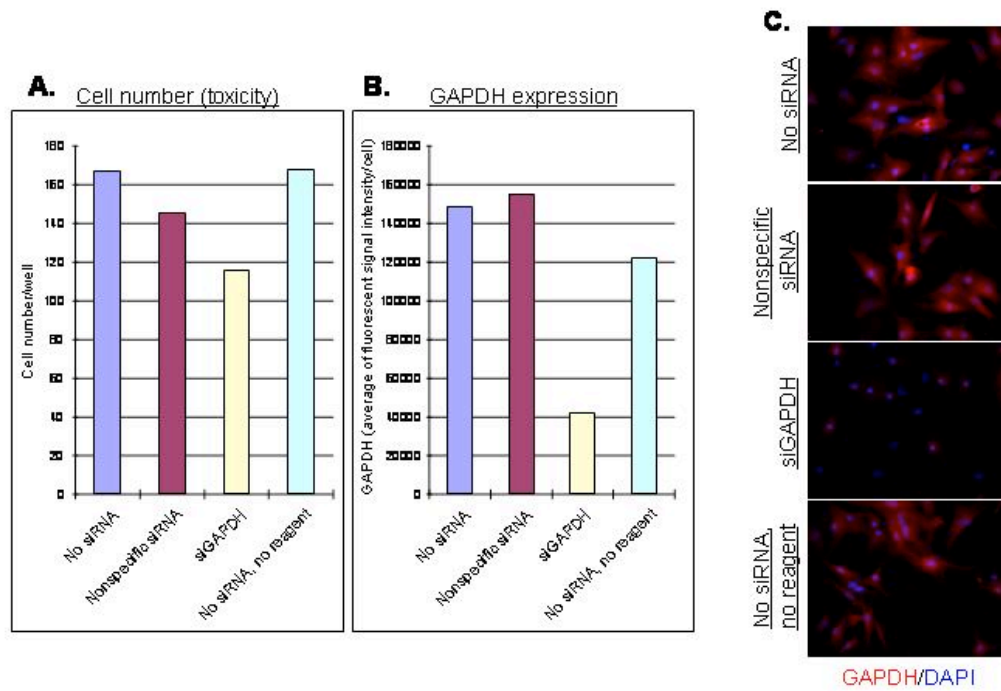


Figure 7: Validation of DharmaFect3 as a transfection reagent for NRVCs (A); Histogram depicting the transfection efficiency of DharmaFect3 based upon the observed GAPDH knock-down in NRVCs by means of a siRNA to GAPDH (B); Representative staining of NRVCs for GAPDH and DAPI (C).

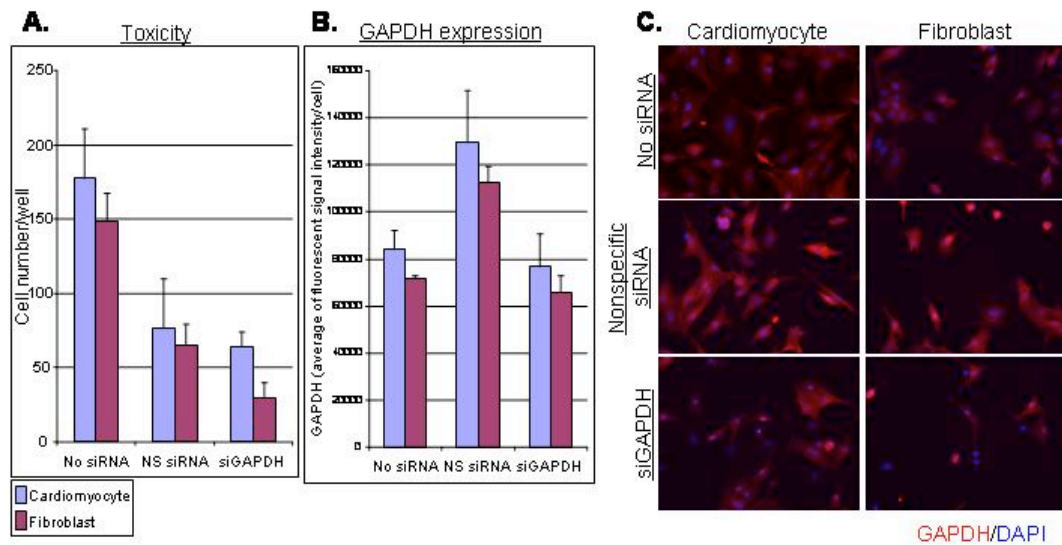


Figure 8: Validation of Lipofectamine 2000 as transfection reagent for NRVCs and NRCFs (A); Bar-graph depicting the transfection efficiency of Lipofectamine 2000 based upon the observed GAPDH knock-down in NRVCs and NRCFs in response to transfection with a siRNA to GAPDH (B). Representative staining of NRVCs and NRCFs for GAPDH expression and DAPI (C).

Reagent	Toxicity	Knockdown efficiency
Lipofectamine RNAi MAX	3	3
Lipofectamine 2000	4	2
TransIT TKO	1	1
TransIT siQuest	1	1
HiPerFect	1	2
DharmaFECT1	2	5
DharmaFECT2	5	3
DharmaFECT3	1	5
DharmaFECT4	3	3

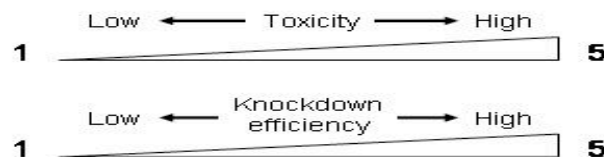


Figure 9: Summary of various transfection reagents compared by their transfection efficiency and toxicity.

Discussion

We optimized the staining and quantitation protocols and also began to establish conditions for reverse transfection of siRNA and miR oligos that yields a high transfection rate and also low toxicity. With further optimization of the automation and verification that knockdown occurs efficiently within the cardiomyocytes, I expect that we will be able to utilize this reagent and the automated technology together to screen libraries of miRNA/siRNA for potential target knock-down effects. Specifically, we will begin by screening a panel of miRs that were identified from the V2 miRNA microarray studies in Chapter 3. We expect that the miRs will work as either agonists of the pathway (mediators of Notch) or as antagonists (feedback inhibitors). Thus, we will test the miRs for the ability to mimic and inhibit Notch-induced cell cycle entry.

In addition, we will plan to screen the Human V3 Anti-miR Inhibitor Library (Ambion Inc.) for specific effects on cell cycle entry visualized by staining with proliferation based markers such as KI-67 and Histone 3-phosphatase. These assays will be performed in hopes corroborating our profiling results and/or identify additional miRs that are involved in the regulation of cell-cycle entry and progression.

Chapter 4--Final Discussion

Our analysis of hESCDCs by means of a miR microarray led to the identification of several miRs that are involved in the differentiation of the hESCs to the cardiomyocyte lineage. We also initiated, on age-matched samples, gene exon array profiling in addition to mass spectrometry analysis of the hESCDCs in relation to the undifferentiated cells. This approach will allow us compare the protein and the transcript levels and correlate this data with specific miR expression patterns in order to filter the list of potential targets (from informatics analyses) to those actually expressed by the cardiomyocytes. The candidate targets will be evaluated in functional studies to confirm that they are the actual targets of the individual miRs. Eventually, knowledge of the miRs and the targets will contribute to a better understanding of how miRs control cardiomyocyte differentiation, proliferation and maturation.

In parallel experiments we determined the miR expression profile of NRVCs that have with activated Notch signaling in relation to NRVCs with a basal level of Notch signaling. The Notch pathway is of interest due to the presence of Notch signaling in the myocardium during development where it plays a potential role in sustaining proliferation of immature cardiomyocytes and its subsequent decrease after birth when the cardiomyocytes become quiescent, and in the adult where it might play a role in regeneration. From the miR studies we have found a list of miRs that have significantly changed in response to the over-expression of Notch signaling. Several of these also had been shown to be directly related to components

of the Notch pathway and their involvement as mediators or feed-back inhibitors of the Notch signaling will be studied using the high throughput assays.

REFERENCES

1. Thom, T., et al., *Heart Disease and Stroke Statistics--2006 Update. A Report From the American Heart Association Statistics Committee and Stroke Statistics Subcommittee*. Circulation, 2006.
2. Beltrami, A.P., et al., *Evidence That Human Cardiac Myocytes Divide After Myocardial Infarction*. The New England Journal of Medicine, 2001. **344**(23): p. 1750-1757.
3. Bearzi, C., et al., *Human Cardiac Stem Cells*. PNAS, 2007. **104**(35): p. 14068-14073.
4. Leri, A., et al., *Human Cardiac Stem Cells*. Microsc Microanal, 2005. **11** (Suppl 2): p. 100-101.
5. Goh, G., et al., *Molecular and phenotypic analyses of human embryonic stem cell-derived cardiomyocytes*. Thromb Haemost, 2005. **94**: p. 728-737.
6. He, J.-Q., et al., *Human Embryonic Stem Cells Develop Into Multiple Types Of Cardiac Myocytes. Action potential Characterization*. Circulation Research, 2003. **93**: p. 32-39.
7. Laflamme, M.A., et al., *Cardiomyocytes derived from human embryonic stem cells in pro-survival factors enhance function of infarcted rat hearts*. Nature Biotechnology 2007.
8. Passier, R., et al., *Increased Cardiomyocyte Differentiation from Human Embryonic Stem Cells in Serum-Free Cultures* Stem Cells, 2005. **23**: p. 772-780.
9. Callis, T.E., J.-F. Chen, and D.-Z. Wang, *MicroRNA's in Skeletal and Cardiac Muscle Development*. DNA and Cell Biology, 2007. **26**(4): p. 219-225.
10. Doench, J.G., C.P. Peterson, and P.A. Sharp, *siRNAs can function as miRNAs*. Genes & Development, 2006. **17**: p. 438-442.
11. Lee, Y.S., et al., *Depletion of Human Micro-RNA miR-125b Reveals That It Is Critical for the Proliferation of Differentiated Cells but Not for the Down-regulation of Putative Targets during Differentiation* The Journal of Biological Chemistry 2005. **280**(17): p. 16635-16641.

12. Cheng, Y., et al., *MicroRNAs Are Aberrantly Expressed in Hypertrophic Heart. Do They Play a Role in Cardiac Hypertrophy?* The American Journal of Pathology, 2007. **170**(6): p. 1831-1840.
13. van Rooij, E., et al., *A signature pattern of stress-responsive microRNAs that can evoke cardiac hypertrophy and heart failure.* PNAS, 2006. **103**(48): p. 18255-18260.
14. van Rooij, E., et al., *Control of Stress-Dependent Cardiac Growth and Gene Expression by a MicroRNA.* Science, 2007. **316**: p. 575-579.
15. Zhao, Y., et al., *Dysregulation of Cardiogenesis, Cardiac Conduction, and Cell Cycle in Mice Lacking miRNA 1-2.* Cell, 2007. **129**: p. 1-15.
16. van Rooij, E., et al., *Control of Stress-Dependent Cardiac Growth and Gene Expression by a MicroRNA.* Science, 2007. **316**: p. 575-579.
17. Zhao, Y., E. Samal, and D. Srivastava, *Serum response factor regulates a muscle-specific microRNA that targets Hand2 during cardiogenesis.* Nature, 2005. **436**: p. 214-220.
18. Schweisguth, F., *Regulation of notch signaling activity.* Curr Biol, 2004. **14**(3): p. R129-138.
19. Rutenberg, J.B., et al., *Developmental patterning of the cardiac atrioventricular canal by Notch and Hairy-related transcription factors.* Development, 2006. **133**(21): p. 1-10.
20. Apelqvist, A., et al., *Notch signaling controls pancreatic cell differentiation.* Nature, 1999. **400**: p. 877-881.
21. Dorsky, R.I., D.H. Rapaport, and W.A. Harris, *Notch inhibits cell differentiation in the Xenopus retina.* Neuron, 1995. **14**: p. 487-496.
22. Jensen, J., et al., *Control of endodermal endocrine development by Hes-1.* Nature Genetics, 2000. **24**: p. 36-44.
23. Rones, M.S., et al., *Serrate and Notch specify cell fates in the heart field by suppressing cardiomyogenesis.* Development (Cambridge, England), 2000. **127**: p. 3865-3876.
24. Wang, S., et al., *Notch receptor activation inhibits oligodendrocyte differentiation.* Neuron, 1998. **21**: p. 63-75.

25. Donovan, J., et al., *Tetralogy of fallot and other congenital heart defects in Hey-2 mutant mice*. *Curr Biol*, 2002. **12**(18): p. 1605-1610.
26. Nemir, M., et al., *Induction of Cardiogenesis in Embryonic Stem Cells via Downregulation of Notch1 Signaling*. *Circulation Research*, 2006. **98**: p. 1471-1478.
27. Li, F., et al., *Rapid transition of cardiac myocytes from hyperplasia to hypertrophy during postnatal development*. *Journal of molecular and cellular cardiology*, 1996. **28**: p. 1737-1746.
28. Burton, P.B., et al., *An intrinsic timer that controls cell-cycle withdrawl in cultured cardiac myocytes* *Developmental Biology*, 1999. **216**: p. 659-670.
29. Winick, M. and A. Noble, *Quantitative changes in DNA, RNA, and protein during prenatal and postnatal growth in the rat*. *Developmental Biology*, 1965. **12**: p. 451-466.
30. Yoo, A.S. and E. Greenwald, *LIN-12/Notch Activation Leads to MicroRNA-Mediated Down-Regulation of Vav in C.elegans*. *Science*, 2005. **310**: p. 1330-1333.
31. Lai, E.C., B. Tam, and G.M. Rubin, *Pervasive regulation of Drosophila Notch target genes by GY-box-, Brd-box-, and K-box-class microRNAs*. *Genes & Development*, 2007. **19**: p. 1067-1080.
32. Kwon, C., et al., *MicroRNA1 influences cardiac differentiation in Drosophila and regulates Notch signaling*. *PNAS*, 2005. **102**(52): p. 18986-18991.
33. Care, A., et al., *MicroRNA-133 controls cardiac hypertrophy*. *Nature Medicine*, 2007. **13**(5): p. 613-618.
34. Thum, T., et al., *MicroRNAs in the Human Heart. A clue to Fetal Gene Reprogramming in Heart Failure* *Circulation*, 2007. **116**: p. 258-267.
35. Sayed, D., et al., *MicroRNAs Play an Essential Role in the Development of Cardiac Hypertrophy*. *Circulation Research*, 2007. **100**: p. 416-424.
36. Chen, J.-F., et al., *The role of microRNA-1 and microRNA-133 in skeletal muscle proliferation and differentiation*. *Nature Genetics*, 2006. **38**(2): p. 228-233.
37. Rand, M.D., et al., *Calcium Depletion Dissociates and Activates Heterodimeric Notch Receptors*. *Molecular and Cellular Biology*, 2000. **20**(5): p. 1825-1835.

38. le Sage, C., et al., *Regulation of the p27^{Kip1} tumor suppressor by miR-221 and miR-222 promotes cancer cell proliferation*. The EMBO Journal, 2007. **26**: p. 3699-3708.
39. Poolman, R.A., et al., *Altered Expression of Cell Cycle Proteins and Prolonged Duration of Cardiac Myocyte Hyperplasia in p27^{Kip1} Knockout Mice*. Circulation Research, 1999. **85**: p. 117-127.
40. Dolt, K.S., et al., *cDNA cloning, gene organization and variant specific expression of HIF-1 α in high altitude yak (Bos grunniens)*. Gene 2007. **386**: p. 73-80.
41. Hua, Z., et al., *MiRNA-Directed Regulation of VEGF and Other Angiogenic Factors under Hypoxia*. PLoS ONE, 2006. **1**(e116): p. 1-13.
42. Gustafsson, M., et al., *Hypoxia requires notch signaling to maintain the undifferentiated cell state*. Development Cell, 2005. **9**: p. 617-628.
43. Tetzlaff, M.T., et al., *Defective cardiovascular development and elevated cyclin E and Notch proteins in mice lacking the Fbw7 F-box protein*. PNAS Early Edition, 2003: p. 1-8.